Shape transition during epitaxial growth of InAs quantum dots on GaAs(001): Theory and experiment

P. Kratzer
Fritz-Haber-Institut der Max-Planck-Gesellschaft, Faradayweg 4–6, D-14195 Berlin, Germany

Q. K. K. Liu
Abteilung Theoretische Physik, Hahn-Meitner-Institut, Glienicker Strasse 100, D-14109 Berlin, Germany

P. Acosta-Diaz, C. Manzano, G. Costantini, R. Songmuang, A. Rastelli, O. G. Schmidt, and K. Kern
Max-Planck-Institut für Festkörperforschung, Heisenbergstrasse 1, D-70569 Stuttgart, Germany
(Received 23 March 2006; published 31 May 2006)

For heteroepitaxial growth of InAs islands on GaAs(001), a transition of shapes is observed experimentally by scanning-tunneling microscopy and analyzed theoretically in terms of the thermodynamic stability of the islands. The experiments show the coexistence of small islands bound predominantly by shallow facets of the {137} family and large islands that show a variety of steeper facets, among them the {101}, {111}, and $\{\bar{1}\bar{1}\bar{1}\}$ orientations. The calculations of island stability employ a hybrid approach, where the elastic strain relief in the islands is calculated by continuum elasticity theory, while surface energies and surface stresses are taken from density-functional theory calculations that take into account the atomic structure of the various side facets, as well as of the InAs wetting layer on GaAs(001). With the help of the theoretical analysis, we interpret the observed coexistence of shapes in terms of a structural phase transition accompanied by a discontinuous change of the chemical potential in the islands. Consequences of this finding are discussed in analogy with a similar behavior of GeSi islands on silicon observed previously.

DOI: 10.1103/PhysRevB.73.205347 PACS number(s): 68.55.Ac, 68.65.Hb, 68.37.Ef, 81.05.Ea

I. INTRODUCTION

Self-organized quantum dots (QDs) grown epitaxially on a semiconductor substrate have been the subject of intense research in recent years. Using molecular beam epitaxy, crystal growers have managed to tailor the size, the shape, and the material composition of such quantum dots according to demands coming from the envisaged application of quantum dots in optoelectronic devices, electronic storage devices, and possibly even future devices for quantum computation.

The size and atomic structure of self-organized QDs is affected both during the first stage of the growth procedure—the deposition of a strained epitaxial layer whose material has a smaller band gap than the substrate and induces the formation of three-dimensional (3D) islands—as well as by the second stage—the overgrowth of the 3D islands by a capping layer of material of again a larger band gap. Moreover, there is experimental evidence that intermixing between the QD material and the matrix occurs to a varying degree, depending on the temperature and deposition rates during growth.[1–3] In the present paper, we restrict ourselves to the simplest case, the growth of free-standing islands consisting of a nominally pure material (InAs) on a GaAs substrate. However, even for this simple case, it is not yet fully understood which principles govern the size and shape of QDs. In earlier works, it has been proposed that the size[4,5] or the shape[6] (or both) are equilibrium properties. Although it appears plausible that materials transport can occur at least over a distance of the island diameter, hence facilitating the equilibration of shapes, as has been seen, for example, in scanning tunnel microscope (STM) images of GeSi islands on Si(001),[7] this fact alone is not a sufficient condition for the QDs actually reaching their equilibrium shape. For example, InAs islands on GaAs(113) were found to be very elongated,[8] an observation that has been attributed to very different growth speeds of the islands' side facets.[9] For InAs quantum dots on GaAs(001), where detailed studies of the theoretically predicted equilibrium shapes have been performed, most experiments reported an aspect ratio considerably lower (between 0.2 and 0.3) than the aspect ratios predicted by theory (between 0.3 and 0.4, see Refs. 6, 10, and 11). This puzzle has been brought a step closer to its solution by the discovery of quantum dots bounded predominantly by shallow {137} facets.[12] QDs with *exclusively* these facets would have a height-to-base (along [110]) ratio of 0.2. Very likely, earlier reports about islands with low aspect ratio were due to the occurrence of this shallow facet, whose atomic structure was not yet resolved in these studies.[13,14] However, there is substantial diversity in the experimental data, and larger aspect ratios have been reported as well, in particular for very big islands obtained by growth with a low deposition rate,[15–17] or by applying post-growth annealing to the samples.[18,19]

It is interesting to note that for GeSi quantum dots on Si a rich variety of shapes has been observed as well; and very recently a shape transition from flat, pyramidal islands to larger islands bounded by a multitude of facets (*domes*) has been established.[20–22] This has motivated proposals that a similar shape transition could take place in the InAs/GaAs system. Early reports of a shape transition[19,23] have been substantiated recently by atomically resolved STM images of InAs quantum dots during various stages of their growth.[24,25] A similar shape transition has been found for island growth on the GaAs(114) substrate as well.[26] Likewise, a bimodal island size distribution has been reported also for InP quantum dots on GaInP[27,28] and on GaAs[29] that could possibly be related to a shape transition.

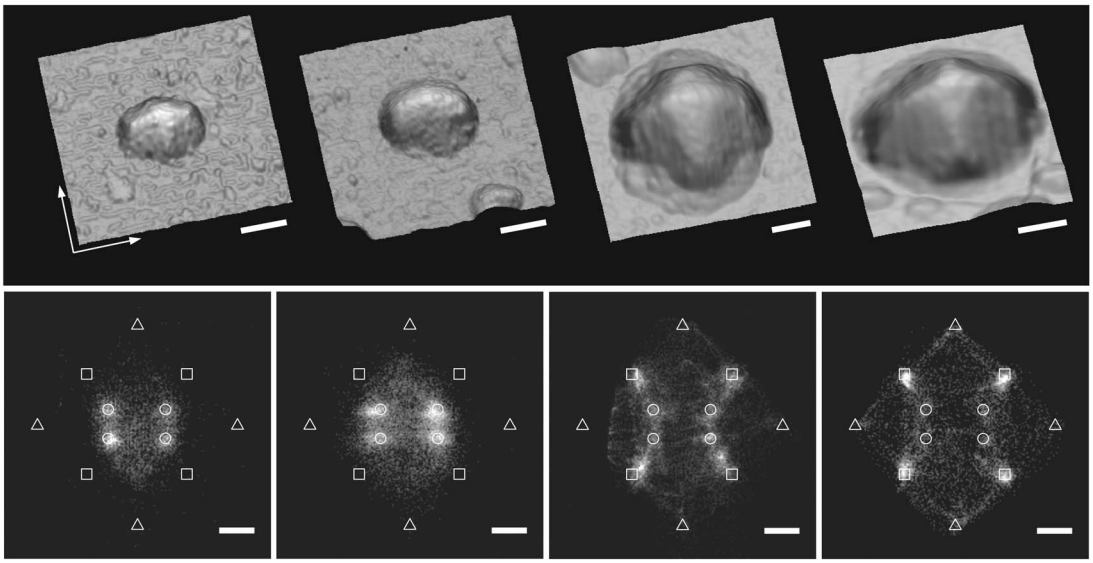

FIG. 1. **Upper row:** STM images of (a) a small pyramidal island, (b) a pyramid at the beginning of the shape transition, a small steeper {011} facet can be recognized on its right side, (c) after the shape transition, with an extended steeper upper part, (d) fully developed dome-shaped island. The scale bar corresponds to 10 nm in each image. **Lower row:** "Facet Plots" corresponding to the islands shown above, i.e., histograms indicating the distribution of normal vectors over the island surface. Normal vectors are represented in two dimensions by the components of the local surface gradient. The scale bar corresponds to 0.5 in each image. The dense clusters of points in the histogram correspond to the predominant facet orientations which are indicated by the corresponding symbols ∘{137}, △{111}, □{101}.

In the present work, we aim at exploring the nature of the shape transition both by experimental growth and characterization of quantum dots by scanning tunneling microscopy (STM), and by a theoretical analysis of the energetics of such a supposed transition. In particular, we want to clarify the role of {137} facets for the shape of InAs quantum dots. These very flat facets had not been considered in the previous calculation[6] of the equilibrium shape of quantum dots. Furthermore, we discuss the implications of the shape transition for the general view of the quantum dot formation as a coarsening process:[22,30] Ross and Tromp have pointed out that a kink in the chemical potential due to, e.g., a shape transition can give rise to anomalous coarsening behavior. This, in turn, might have a significant effect on the island size distribution and can give rise to an unusually sharp peak (compared to Ostwald ripening), a feature that is crucial for numerous applications. In support of these considerations, our calculations show that indeed a discontinuity of the chemical potential in InAs quantum dots occurs as soon as steeper {101} facets appear on the shallow {137} facets in the course of island growth.

In the following, we shall first describe the experimental techniques and results. Secondly, the hybrid approach for calculating the thermodynamic stability of the islands will be reviewed. We discuss the results of the calculations for the chemical potential of indium atoms, for the overall energy gain due to island formation, and for the optimum aspect ratio of the islands. Finally, we conclude by discussing the implications of the observed shape transition for the growth kinetics of island ensembles.

II. EXPERIMENTAL

The quantum dots were grown by depositing 1.8 monolayers (MLs) of InAs on a GaAs(001) substrate under conditions similar to those described in Ref. 31. Atomic In was evaporated by molecular beam epitaxy at a rate of 0.008 ML/s under an As_4 beam-equivalent pressure of 8×10^{-6} mbar and at a substrate temperature of 500 °C. After cooling, the samples were transferred under ultrahigh vacuum conditions to an STM and there imaged at room temperature.

The samples show the coexistence of islands with different shapes with a predominance of small shallow islands mainly delimited by {137} facets (*pyramids*) and larger multifaceted islands that include {101} and {111} facets (*domes*).[31] Other islands with shapes and sizes intermediate between those of pyramids and domes are observed as well, but with a much lower frequency. The upper row in Fig. 1 displays representative STM images of the different island types and exemplifies the transformation path that growing pyramids undergo when they evolve into domes. While in Fig. 1(a) a pristine {137} pyramid can be recognized, the island in Fig. 1(b) has started to develop a small (011) facet in its upper-right side. Figure 1(c) represents a later stage of the shape transition in which extended {101} facets have appeared on all sides of the island and two small $\{\bar{1}\bar{1}\bar{1}\}$ facets have formed along $[\bar{1}10]$. Finally, in Fig. 1(d) a mature dome is shown which displays also {111} facets along [110]. We notice that in very few cases we also found domes where the small shallow facets recognizable at the island top and bottom in Fig. 1(d) had completely disappeared.

The transition from shallower to steeper facets can be quantitatively followed in the lower row of Fig. 1 where the corresponding two-dimensional (2D) histograms of the normal vector over the island surface (*facet plots*[32]) are displayed. The different clusters of points indicate the existence of well-defined facets that can be precisely determined

through the position of the center of mass of the cluster. Figures 1(e)–1(h) show that the shape transformation mainly happens through the successive evolution of {101} and {111} facets at the expense of {137} ones.

Figure 1 and the similar results recently published by Xu *et al.*, Ref. 25, clearly demonstrate that the pyramid-to-dome transition in the InAs/GaAs(001) systems is almost identical to the corresponding transition occurring during the growth of Ge on Si(001).[21] This analogy substantiates the claim that very similar microscopic processes must govern the evolution of QDs in these two material systems.[24]

III. CALCULATIONS

We analyze the energy gain associated with the formation of three-dimensional islands on the wetting layer by employing the hybrid approach, introduced in Ref. 10, and extended to include surface stress in Ref. 6. The total energy gain is divided into a contribution originating from bulk strain relaxation, E_{relax}, and terms accounting for the additional formation of island facets, E_{surf}, and edges, E_{edge}.

$$E_{\mathrm{tot}} = E_{\mathrm{relax}} + E_{\mathrm{surf}} + E_{\mathrm{edge}}. \tag{1}$$

We stress that, in each term, the energy *difference* between a 3D island, and a homogeneous planar InAs film of the same volume is considered.

The treatment of the first term, the elastic relaxation, is done entirely within classical continuum elasticity theory. For the 3D islands of various shapes, we have used a finite element method. Results of such calculations for uncapped InAs islands on GaAs substrate have been reported previously.[6,10] These, together with similar calculations done for InP islands on GaP substrates,[35] have demonstrated the applicability of the results to nanostructures. The explicit values of the moduli of elasticity c_{11}, c_{12}, and c_{44} of InAs and GaAs are found in the literature.[6,34] The mismatch between InAs and GaAs that gives rise to the elastic energies is $\alpha := (a_{\mathrm{GaAs}} - a_{\mathrm{InAs}})/a_{\mathrm{InAs}} = -6.7\%$, where a_{GaAs} and a_{InAs} are the lattice constants of GaAs and InAs, respectively. We have used the commercial product MARC[33] to perform finite-element calculations for the elastic energy stored both in the substrate and the epitaxial 3D island, $E^{\mathrm{is}}_{\mathrm{relax}}$. The size of the substrate is suitably chosen according to the density of islands seen in the experiments. Periodic boundary conditions were applied to the side planes of the material in the simulation. The distribution of the eight-node hexahedral finite elements was such that the number of finite elements was increased in the parts of the island where the elastic energy density was large until we could arrive at an estimate of the accuracy of 5%.

For the situation of a homogeneous planar film, the elastic energy per unit volume can be given in analytical form,

$$\epsilon_{\mathrm{film}} = \left(c_{11} + c_{12} - 2\frac{c_{12}^2}{c_{11}} \right) \alpha^2. \tag{2}$$

The energy of relaxation, E_{relax} of Eq. (1), is the difference between the remaining bulk strain energy stored in the island plus the substrate after relaxation, $E^{\mathrm{is}}_{\mathrm{relax}}$, and the energy in an equivalent unstrained volume V of a fully strained epitaxial InAs film on GaAs, $\epsilon_{\mathrm{film}} V$.

Calculation of the second and third term in Eq. (1) requires knowledge about the detailed atomic structure, and hence density functional theory (DFT) calculations for the surface energies of (reconstructed) surfaces are needed. At present, we neglect the third term in Eq. (1), the energy of edges, due to lack of knowledge about the atomic reconstruction near the edges. This approximation is justified for not too small islands, as those observed in the present experiments, since the ratio of edges relative to a flat facet area decreases with increasing island size. For the surface energies, results of DFT calculations within the local-density approximation are available in the literature for low-index facets of InAs.[6] For nonstoichiometric surfaces, the surface energy is a function of the chemical environment, which is described by the chemical potential of arsenic, μ_{As}, in the growth apparatus, corresponding to the experimental choice of temperature and arsenic partial pressure during growth. In the following, we model moderately arsenic-rich conditions, using $\mu_{\mathrm{As}} = \mu_{\mathrm{As(bulk)}} - 0.2$ eV in compliance with earlier work.[11] This value is close to the experimental conditions for growing the samples shown in Fig. 1.[36] In experimental terms, $\mu_{\mathrm{As}} = \mu_{\mathrm{As(bulk)}} - 0.2$ eV corresponds to InAs deposition at temperatures slightly above the transition of the GaAs(001) substrate from the $c(4\times4)$ to the $\beta2(2\times4)$reconstruction,[37] and leads to the (re)appearance of a (2×4) pattern on the wetting layer immediately before the 2D-3D growth transition. A detailed study of the structure of the wetting layer by means of DFT calculations[38] shows that the wetting layer, for an In deposition of more than 1.75 ML and moderately arsenic-rich conditions, displays a (possibly disordered) $\alpha2(2\times4)$ reconstruction. To complement the calculated data for low-index InAs surfaces, we have performed DFT calculations for the surface energy of InAs(137) using the same methodology as described in Refs. 6 and 39 [note that the basic structural unit of the (137) surface is the elementary building block of the more complex (2 5 11) and (3 7 15) surfaces described previously in Ref. 39].

Since the (137) facet appears at the base of the experimentally observed dome-shaped QDs and hence may be highly strained, we calculate the dependence of its surface energy, $\gamma^{(137)}(\epsilon)$, on strain, ϵ. To this end, we have performed DFT calculations for slabs under biaxial strain, while the surface could relax freely in the direction of the surface normal. Results of these calculations are shown in Fig. 2. We find that the surface energy is significantly reduced under compressive biaxial strain. This finding is in close analogy to GeSi QDs on Si(001), where it has been shown that the surface energy of the (105) side facet is also strongly reduced by strain.[40–43] To capture the strain dependence, a parametrization by a third-order polynomial is used for the {137} facets. For the other facets forming the steep upper part of the QD the surface strain is small and can be taken into account by a linear correction proportional to the intrinsic surface stress, $\sigma^{(i)}$, following earlier work by Moll *et al.* (Ref. 6)

$$\gamma^{(i)}(\epsilon) = \gamma^{(i)}(\epsilon = 0) + \mathrm{Tr}(\sigma^{(i)}\epsilon^{(i)}). \tag{3}$$

For a numerical evaluation of $\gamma^{(i)}(\epsilon)$, the two in-plane components of the strain on each facet, averaged over the facet

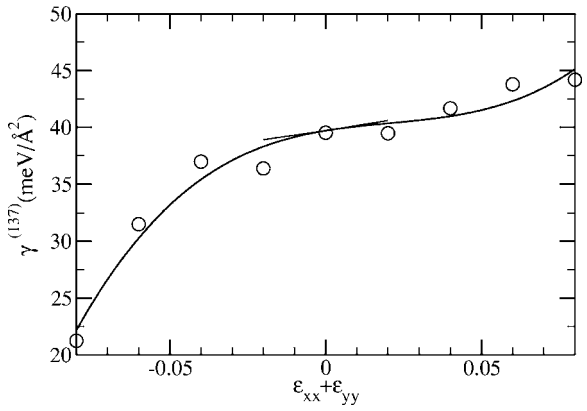

FIG. 2. Surface energy γ of the InAs(137) surface as a function of strain, ϵ, per unit surface area (of the unstrained material).

area, are taken from the finite-element calculations. We find the two components to be rather similar, which justifies the approximative use of an isotropic stress tensor in Eq. (3). Finally, the term E_{surf} in Eq. (1) is calculated as follows:

$$E_{\text{surf}} = \sum_i \gamma^{(i)}(\epsilon^{(i)})A^{(i)} - \gamma^{(0)}A^{(0)},$$

where $\gamma^{(i)}(\epsilon^{(i)})$ and $A^{(i)}$ denote the surface energies and surface areas of the ith side facet of the QD. The numerical values of $\gamma^{(i)}$ and $\sigma^{(i)}$ are adopted from Fig. 2 and from Ref. 6, Table II. $A^{(0)}$ denotes the QD base area, and $\gamma^{(0)}$ is the energy per area of the wetting layer, including both surface and interface contributions, but excluding the strain energy stored in the wetting layer [which is treated separately by the term ϵ_{film}, cf. Eq. (2)]. Numerically, the value $\gamma^{(0)}(\mu_{\text{As}} = \mu_{\text{As(bulk)}} - 0.2\ \text{eV}) = 41.2\ \text{meV/Å}^2$ is used, which has been determined from DFT calculations.[38]

IV. RESULTS AND DISCUSSION

In the following, we suggest a kinetic pathway for the transition from small to large InAs QDs and explore its energetic implications. Since the shape transition is a dynamic nonequilibrium phenomenon involving up to 10^5 atoms, it is very difficult to describe it using results from theoretical calculations of equilibrium properties. We rather need to use experimental information about intermediate shapes as input for our analysis, augmented by the guiding principle that changes of the QD shape occur predominantly through surface mass transport. This implies that a later shape during the growth transition results from an earlier shape by adding material to the side facets (by a layer-by-layer growth on these facets). This is particularly plausible at the growth temperatures used for our experiments and implies that the material already incorporated into a complete side facet will remain there and is no longer available for growth or reshaping of the QDs.

Our description of the shape transition, inspired by the experimental observations shown in Fig. 1, is outlined in the sequence of pictures in Fig. 3: We start from the flat shape bounded predominantly by the {137} facets observed experimentally, and proceed by adding a steeper top part delimited by low-index facets whose size continuously increases from Figs. 3(b)–3(e). For the construction of the shape, we use the guiding principle (evidenced in Ref. 44) that, whenever shallow facets exist at all as part of the equilibrium shape, they must appear both in the top part and at the foot of the quantum dot. This is in line with the experimental observation, Fig. 1(c), where, in addition to shallow facets at the top, the QD is found to be surrounded by a rim of material with the same slope as the top facet.[24,31]

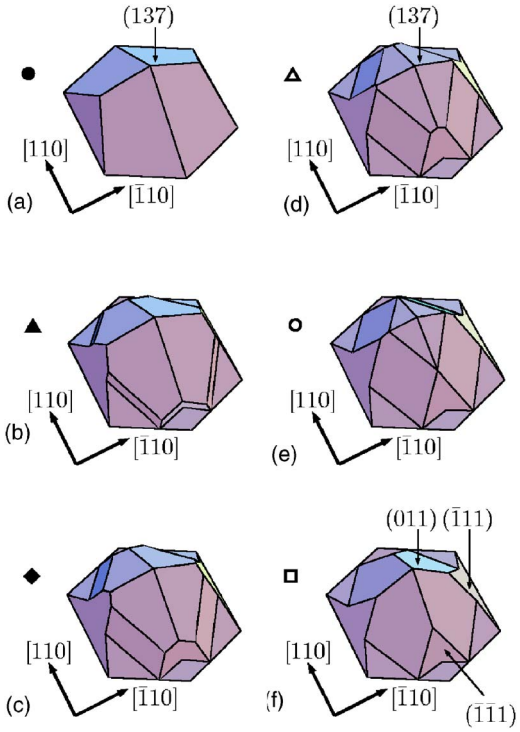

FIG. 3. (Color online) Proposed sequence of shapes for the growth of InAs quantum dots on GaAs(001). Small quantum dots, (a), are bounded by {137} and {$\bar{1}\bar{1}\bar{1}$} facets. Growth proceeds mostly through layer-by-layer growth on the {137} facets; however, the newly grown layers do not make contact with the (001) substrate (b). As a result, {110} and {111} facets develop at the lower end of the added layers, giving the quantum dot an increasingly steeper appearance (c)–(e). Eventually, a sharp tip could possibly develop if growth of the {110} facets extends to the top (f).

We note that in order to facilitate the calculations, we have assumed somewhat simpler island shapes compared to the experimental ones. For example, we have neglected the small shallow {$\bar{1}$35} and {$\bar{1}$12} facets that have been recently reported for the first stages of the QD evolution.[25] Nevertheless, we believe that this simplification does not substantially modify the key aspects of the shape transition.

A. Energy release by quantum dot formation

For all the shapes calculated, we find that the first term in Eq. (1) is an energy gain, i.e., the islands stabilize themselves by strain relief compared to the homogeneously strained film. It can be shown within continuum elasticity theory that

the bulk strain relief (disregarding island-island interaction and strain relief due to edge discontinuities) scales proportional to the volume of the QD. On the other hand, the second term in Eq. (1), due to the creation of side facets, is found to be an energetic cost for all calculated shapes. As a surface term, it scales like $V^{2/3}$ to leading order [i.e., disregarding the renormalization of surface energies due to strain, cf. Eq. (3)]. We make use of this scaling relation to extend our results, calculated for a particular shape and size, to quantum dots of the same shape, but arbitrary size. The gain due to strain relief, E_{relax}, being a volume effect, ultimately becomes dominant for the larger QDs. Using the scaling relation

$$E_{\mathrm{tot}} = e_{\mathrm{relax}} V + e_{\mathrm{surf}} V^{2/3} \tag{4}$$

enables us to extend our results, calculated for a particular quantum dot size, to any size of the QD, where $e_{\mathrm{relax}} = E^{\mathrm{is}}_{\mathrm{relax}}/V - \epsilon_{\mathrm{film}} < 0$ and $e_{\mathrm{surf}} = E_{\mathrm{surf}}/V^{2/3} > 0$ are shape-dependent quantities calculated within continuum elasticity theory and within DFT, respectively.

While the above results are strictly valid only for pure InAs QDs, a generalization to the more realistic case of intermixed (In,Ga)As quantum dots is not straightforward. The lower surface energy of InAs compared to GaAs causes InAs surface segregation in alloyed islands. As a consequence, the surface term [e_{surf} in Eq. (4)] calculated in this paper should be valid also for more realistic QDs. The situation is clearly different for the bulk strain relaxation. As long as the (In,Ga)As alloy is uniformly distributed within the island, the only difference with the energy values calculated here would be a reduced lattice mismatch α and therefore, from Eq. (2), a smaller elastic energy per unit volume. The experimentally reported island compositions are, however, quite inhomogeneous, with an increasing indium concentration in the growth direction.[1–3] While the gallium concentration in the pyramid-shaped island base is significant, the dome-shaped upper part is highly indium rich. This will certainly affect the strain relief [e_{relax} in Eq. (4)], but we expect this to be a second-order effect, since e_{relax} approaches a constant for the larger islands.

B. Chemical potential of In atoms in the QD

Previous theoretical work[11] has given evidence that for a given amount of material the 3D islands during their growth stage are fed by material diffusing towards the island from the wetting layer around it. This idea has been experimentally confirmed both indirectly by arguments of mass conservation,[45] as well as by direct observation of the erosion of steps near QDs.[46,47] Under conditions where the mass transport occurs sufficiently close to equilibrium, it can be described as being driven by a difference of chemical potential $\Delta\mu_{\mathrm{In}}$ between the InAs species in the island and in the surrounding wetting layer: As long as the chemical potential of an atom attached to the quantum dot is lower than the chemical potential of the adatom lattice gas, the QD will proceed to grow; else its growth will stop. In the following, we will derive the relevant chemical potential difference as a function of QD size and shape from our hybrid approach.

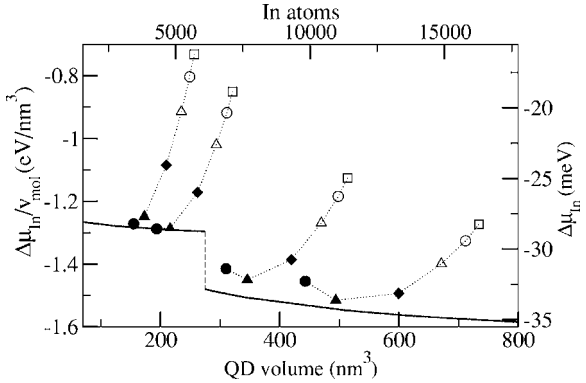

FIG. 4. Chemical potential of In atoms in quantum dots of various fixed base areas, as a function of the dot volume. The curves, from upper left to lower right, correspond to quantum dots with a base diameter in [110] direction of 19.8, 24.7, 39.6, and 56.6 nm, respectively. The symbols along the curves refer to the different shapes shown in Fig. 3. For quantum dots of small base area, adding material on top of the pyramid, Fig. 3(a), would result in an increase of chemical potential and hence does not occur spontaneously. For quantum dots with a base length larger than 30 nm, however, a transition from the shape Fig. 3(a) to Fig. 3(b) becomes a spontaneous process accompanied by a lowering of $\Delta\mu_{\mathrm{In}}$ [dotted lines, Eq. (6)]. The unconstrained chemical potential (solid line) shows an abrupt drop at the growth transition.

For the usual definition of the chemical potential, allowing for an unconstrained variation of shape with size, differentiation of Eq. (4) with respect to the number of In atoms, N_{In} (proportional to V) yields a monotonously decreasing function. It is shown as a solid line in Fig. 4 and will be discussed further below. However, as we indicated in the preceding section, it is more relevant to consider a situation where attachment of new material at the foot of the quantum dot has stopped to occur due to the highly compressive strain that makes attachment of InAs in this region highly energetically unfavorable (see, e.g., Ref. 48, although the authors, somewhat paradoxically, assume that facet growth would initiate in this highly strained region). There is experimental support for such a scenario, which has been put forward by Madhukar and co-workers under the term *punctuated island growth*.[23] Recently, Montalenti *et al.* (Ref. 21) and Xu *et al.* (Ref. 25) have employed similar considerations to analyze their experimental data. Mathematically, the chemical potential can be obtained in this case from the variation of the free enthalpy under the constraint of fixed base area of the quantum dot. As we will see below, the chemical potential difference

$$\Delta\mu_{\mathrm{In}} = \left.\left(\frac{\partial \Delta G}{\partial N_{\mathrm{In}}}\right)\right|_{p,T,A^{(0)}} \tag{5}$$

$$\approx \left.\frac{\partial E_{\mathrm{tot}}}{\partial N_{\mathrm{In}}}\right|_{A^{(0)}} = \mathrm{v}_{\mathrm{mol}} \left.\frac{\partial \mathrm{E}_{\mathrm{tot}}(\mathrm{A}^{(0)})}{\partial \mathrm{V}(\mathrm{A}^{(0)})}\right|_{A^{(0)}} \tag{6}$$

defined with *the constraint of fixed base area* $A^{(0)}$ is generally a nonmonotonous function of V. Here, $\mathrm{v}_{\mathrm{mol}}$ is the vol-

ume of an InAs pair in the InAs crystal. Moreover, in going from Eq. (5) to Eq. (6), we have assumed that vibrational and configurational entropy contributions to ΔG largely cancel when considering differences, and hence these contributions can be neglected.

To be specific, we consider the situation where further growth of the QD is possible only by incomplete facet layer growth: At first, a small island, of the shape shown in Fig. 3(a), will grow in layer-by-layer growth mode on the {137} facets, thus reproducing its shape. As the most likely growth scenario, we consider that the facet layers start to grow from the island top and fill the facet by growing downward. At a later stage, layer growth stops before the growing facet layer touches down to the substrate [or only reaches it at a single point, as shown in Fig. 3(b)]. While more and more incomplete {137} facet layers grow from top to bottom, steeper facets of the {110}, {111}, and $\{\bar{1}\bar{1}\bar{1}\}$ families develop at lower terminating edges of the incomplete facets. Figures 3(c)–3(f) are a schematic representation of this growth sequence. In the language of layer-by-layer growth, the appearance of steeper facets can be interpreted as step bunching. Indeed, for Ge islands on Si, an analogous discussion in terms of stepped side facet growth has been given in Ref. 21. The growth scenario of Fig. 3, evaluated for fixed base area $A^{(0)}$, defines a unique relation $V(A^{(0)})$, which enables us to evaluate the derivative in Eq. (6).

Figure 4 displays both the unconstrained chemical potential (solid line), and the chemical potential for constrained growth of islands with a given base area (dotted lines). The latter was obtained by inserting the scaling relation, Eq. (4), for $E_{\mathrm{tot}}(A^{(0)})$ into Eq. (6), and taking the derivative under the constraint of fixed base area. While the unconstrained chemical potential decreases monotonously, the constrained chemical potential is found to increase for the two smallest base areas shown. The latter finding indicates that there is no driving force for a spontaneous transition of the island shape in these cases, i.e., the shape of Fig. 3(a) is stable for small base areas, and would reproduce itself in a layer-by-layer growth mode on the side facets. For islands with larger base areas, however, the constrained chemical potential decreases when growth proceeds from Fig. 3(a) to Fig. 3(b) (compare the filled circles and filled triangles in Fig. 4). This implies that layer growth on the {137} facets becomes incomplete, and a band of steeper {101} facets develops spontaneously. The shape transition is defined by this initial decrease in the constrained chemical potential. For the conditions of this study ($\mu_{\mathrm{As}}=\mu_{\mathrm{As(bulk)}}-0.2$ eV), the shape transition occurs for a volume of about 270 nm,[3] a base diameter of about 30 nm, or 6000 In atoms and 6000 As atoms in the island. We note that these numerical values may vary depending on growth temperature, arsenic partial pressure, and the degree of actual intermixing between InAs and GaAs in the QD. Although this implies that a direct comparison of the calculated values with experiments has to be taken cautiously, the values of the transition volume that we found in our measurements agree reasonably well with the theoretical ones. The fact that the transition is spontaneous only above a specific island size can be expressed also in another way: Introducing the band of {101} facets is energetically favorable only if they have a minimum size, i.e., if the island has some minimum base length. For smaller islands, the energetic cost of introducing these facets is not yet counterbalanced by the energy gain of strain relief in the upper part of the island.

The unconstrained chemical potential (solid line in Fig. 4) shows an abrupt drop at the shape transition. This behavior brought out by our hybrid approach for the InAs/GaAs(001) islands conforms with the results of a simpler continuum treatment for GeSi islands on Si(001):[30] Both in this study and in our work, a discontinuity of the chemical potential occurs during island evolution. The consequences of this finding for the growth kinetics have been worked out.[30,49] In brief, it gives rise to an anomalous island size distribution characterized by a few islands that have passed the transition point and continue to grow quickly, while a large number of smaller, pyramidal islands are left behind in their evolution. While the smallest islands shrink (as seen in Ref. 7) and are eventually consumed by the large dome-shaped islands, the remaining pyramids show a narrow distribution of sizes peaked slightly below the transition point. Thus the spontaneous transition to large dome-shape islands triggers anomalous coarsening of the overall island population. In this case, a narrower island distribution than expected for conventional (Ostwald) coarsening kinetics results. We expect a similar anomalous kinetics to be operative in the InAs/GaAs(001) system. Due to our atomistic treatment of the surface energies, we can identify the incomplete facet growth on the {137} side facets of the InAs QDs and the appearance of steeper {101} factes as the microscopic cause for the anomalous coarsening kinetics.

C. Shape of equilibrated QDs

If one considers a single quantum dot as an isolated system (rather than in equilibrium with the wetting layer), the stability of the QD is characterized by the energy per atom, or likewise, per volume, E_{tot}/V. Such a theoretical description allows for *arbitrary* changes of the QD shape and is appropriate for modeling annealing experiments without material deposition, where the influx of atoms to the islands is much smaller than during growth. Making contact to previous studies,[6,11] the quantity E_{tot}/V is evaluated and compared for different shapes and sizes. The curves plotted in Fig. 5 were obtained by evaluating Eq. (4) for the various shapes of QDs shown in Fig. 3. The asymptotic energy gain in the limit of large QDs, dominated by strain relief, is maximum for the fully developed dome shape. For small islands, however, the flat pyramid is energetically favorable, due to its low cost in terms of surface energy. The shallow {137} side facets increase the surface area only moderately compared to the base area $A^{(0)}$ of the QD. Moreover, the high surface strain on these facets lowers their surface energies considerably, as seen from Fig. 2. Going from small to large QD volumes, the energetically most favorable shape runs through the sequence depicted in Figs. 3(a)–3(e). The lowest-energy pathway for QD growth, within the family of shapes given by Fig. 3, corresponds to the lower convex envelope of the curves for the individual shapes. The arrow in Fig. 5 indicates a cusp in this curve at $V=270$ nm^3 associated with the

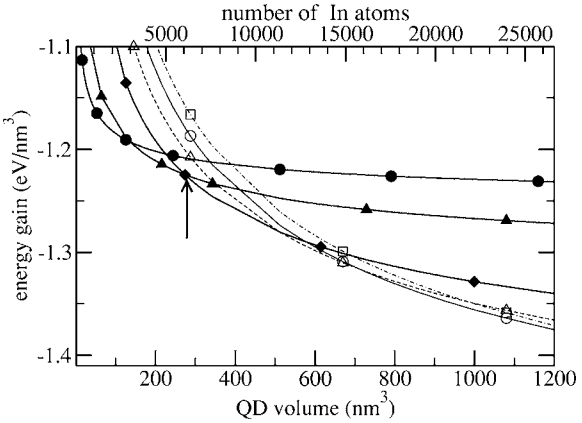

FIG. 5. Energy gain per volume for the formation of quantum dots of different shapes, as shown in Fig. 3, as a function of the dot volume. The symbols refer to the shapes labeled (a)–(f) in Fig. 3. The lowest-energy pathway for quantum dot growth within the given family of shapes is described by the lower convex envelope of the individual curves. The arrow marks the shape transition point.

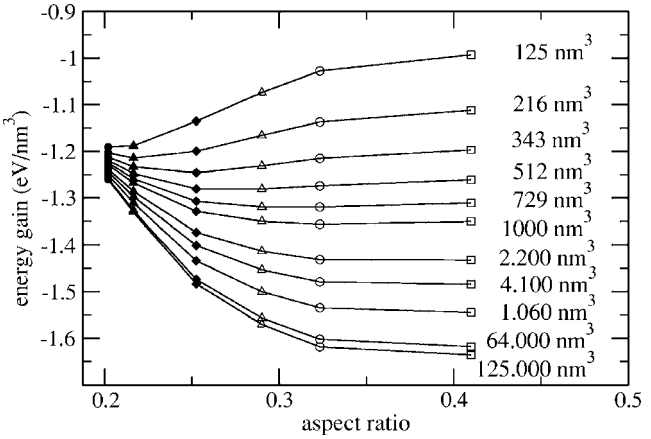

FIG. 6. Energy gain per unit volume for a quantum dot formed from a given amount of material, but with no restrictions on its shape. On the abscissa, the shapes displayed in Fig. 3 are represented by their aspect ratio (height:base diameter). The curves, from top to bottom, correspond to an increasing amount of material (volume), as specified by the labels. While for small quantum dots (uppermost curve) the flat pyramid of Fig. 3(a) is energetically preferable, quantum dots in later stages of their growth prefer a domelike shape.

shape transition. Since only a discrete set of shapes has been calculated, Fig. 5 alone would not warrant such a conclusion. However, the analysis of growth with a fixed base area in the previous section puts us in a position to conclusively identify the shape transition point. The cusp in the lower convex envelope in Fig. 5 gives rise to the discontinuous drop of the unconstrained chemical potential at the transition seen in Fig. 4. It is interesting to note that the shape of Fig. 3(b) (filled triangles) appears in Fig. 5 already before the shape transition, while its first appearance is indicative of the transition in Fig. 4. This is due to the different restrictions imposed in both treatments: Dropping the constraint of the fixed base area, i.e., allowing for the relocation of material from the QD foot to the top facets, stabilizes the shape of Fig. 3(b) already at an earlier stage. Compared to previous work[11] assuming a QD shape bound by low-index facets *only*, the lower convex envelope obtained in the present study has a smaller energy per volume. Thus we have demonstrated that the occurrence of the high-index {137} facets indeed leads to an enhanced stability of the QDs, which gives additional support to the choice of shapes in Fig. 3 originally inspired by the experiment.

The transition from the flat to a domelike shape is clearly visible when the energy gain E_{tot}/V is plotted for a fixed amount of material as a function of a variable parametrizing the shape transition. In Fig. 6, we use the aspect ratio (ratio of height to base diameter, measured along [110]) as a descriptor of the shape. Clearly, dots of a small volume are seen to have a minimum of the energy per particle for the flat pyramidal shape, while very large QDs, of a size larger than 1000 nm^3, favor a very steep shape with an aspect ratio in excess of 0.4, [see for example Fig. 3(f)]. Between these two extremes, islands with an aspect ratio in the range of 0.29–0.33 are found to be the energy minimum of the moderately larger QDs of the typical sizes observed in the experiment, with a volume up to about 1000 nm^3, or up to some 22 000 indium atoms. Thus, the range of aspect ratios for small and medium-sized QDs found in our present study is in much better agreement with experiment than previous theoretical models.[6,11]

V. CONCLUSIONS

In a combined work comprising STM measurements of InAs islands grown by molecular beam epitaxy and calculations of the thermodynamic stability of these islands, we provide evidence for a shape transition in InAs/GaAs(001) heteroepitaxy. For small island sizes, flat pyramids dominated by {137} facets are energetically favorable. Density-functional calculations of the surface energy and surface stress of these facets show that their appearance is favored by the pronounced lowering of the (137) surface energy on the compressively strained side facets of the InAs QDs. For larger islands, a higher aspect ratio is found to be preferable due to more efficient strain relaxation in the steep part of the island. Hence there is a thermodynamic driving force for developing a domelike shape on top of a flat base as the island grows larger. Furthermore, our theoretical analysis shows that the change of the island shape can be understood in analogy to a structural phase transition with an abrupt drop of the chemical potential at the transition point, with important consequences for the growth kinetics of the island ensemble as a whole.

ACKNOWLEDGMENTS

P.K. would like to thank K. Jacobi for valuable discussions and for providing experimental data prior to publication. This work was supported by the Deutsche Forschungsgemeinschaft within SFB296 and by the European Network of Excellence SANDiE.

[1] N. Liu, J. Tersoff, O. Baklenov, A. L. Holmes, Jr., and C. K. Shih, Phys. Rev. Lett. **84**, 334 (2000).
[2] I. Kegel, T. H. Metzger, A. Lorke, J. Peisl, J. Stengl, G. Bauer, J. M. Garcia, P. M. Petroff, Phys. Rev. Lett. **85**, 1694 (2000); I. Kegel, T. H. Metzger, A. Lorke, J. Peisl, J. Stengl, G. Bauer, K. Nordlund, W. V. Shoenfeld, P. M. Petroff, Phys. Rev. B **63**, 035318 (2001).
[3] D. M. Bruls *et al.*, Appl. Phys. Lett. **81**, 1708 (2002); *ibid.* **82**, 3758 (2003).
[4] V. A. Shchukin, N. N. Ledentsov, P. S. Kop'ev, and D. Bimberg, Phys. Rev. Lett. **75**, 2968 (1995).
[5] I. Daruka, J. Tersoff, and A. L. Barabási, Phys. Rev. Lett. **82**, 2753 (1999).
[6] N. Moll, M. Scheffler, and E. Pehlke, Phys. Rev. B **58**, 4566 (1998).
[7] A. Rastelli, M. Stoffel, J. Tersoff, G. S. Kar, and O. G. Schmidt, Phys. Rev. Lett. **95**, 026103 (2005).
[8] Y. Temko, T. Suzuki, and K. Jacobi, Appl. Phys. Lett. **82**, 2142 (2003).
[9] Y. Temko, T. Suzuki, P. Kratzer, and K. Jacobi, Phys. Rev. B **68**, 165310 (2003).
[10] E. Pehlke, N. Moll, A. Kley, and M. Scheffler, Appl. Phys. A **65**, 525 (1997).
[11] L. G. Wang, P. Kratzer, N. Moll, and M. Scheffler, Phys. Rev. B **62**, 1897 (2000).
[12] J. Márquez, L. Geelhaar, and K. Jacobi, Appl. Phys. Lett. **78**, 2309 (2001).
[13] Y. Hasegawa, H. Kiyama, Q. K. Xue, and T. Sakurai, Appl. Phys. Lett. **72**, 2265 (1998).
[14] H. Lee, W. Y. R. Lowe-Webb, and P. C. Sercel, Appl. Phys. Lett. **72**, 812 (1998).
[15] K. Zhang, C. Heyn, W. Hansen, T. Schmidt, and J. Falta, Appl. Phys. Lett. **76**, 2229 (2000).
[16] K. Zhang, C. Heyn, W. Hansen, T. Schmidt, and J. Falta, J. Cryst. Growth **227/228**, 1020 (2001).
[17] G. Costantini, C. Manzano, R. Songmuang, O. G. Schmidt, and K. Kern, Appl. Phys. Lett. **82**, 3194 (2003).
[18] O. G. Schmidt *et al.*, Surf. Sci. **514**, 10 (2002).
[19] H. Saito, K. Nishi, and S. Sugou, Appl. Phys. Lett. **74**, 1224 (1999).
[20] G. Medeiros-Ribeiro, A. M. Bratkovski, T. I. Kamins, D. A. A. Ohlberg, and R. S. Williams, Science **279**, 353 (1998).
[21] F. Montalenti *et al.*, Phys. Rev. Lett. **93**, 216102 (2004).
[22] F. M. Ross, J. Tersoff, and R. M. Tromp, Science **286**, 1931 (1999).
[23] I. Mukhametzhanov, Z. Wei, R. Heitz, and A. Madhukar, Appl. Phys. Lett. **75**, 85 (1999).
[24] G. Costantini *et al.*, Appl. Phys. Lett. **85**, 5673 (2004).
[25] M. C. Xu, Y. Temko, T. Suzuki, and K. Jacobi, J. Appl. Phys. **98**, 083525 (2005).
[26] M. C. Xu, Y. Temko, T. Suzuki, and K. Jacobi, Phys. Rev. B **71**, 075314 (2005).
[27] N. Carlsson *et al.*, J. Cryst. Growth **156**, 23 (1995).
[28] J. Porsche, A. Ruf, M. Geiger, and F. Scholz, J. Cryst. Growth **195**, 591 (1998).
[29] J. Johansson, W. Seifert, T. Junno, and L. Samuelson, J. Cryst. Growth **195**, 546 (1998).
[30] F. M. Ross, J. Tersoff, and R. M. Tromp, Phys. Rev. Lett. **80**, 984 (1999).
[31] G. Costantini *et al.*, J. Cryst. Growth **278**, 38 (2005).
[32] A. Rastelli and H. von Känel, Surf. Sci. **515**, L493 (2002).
[33] *MARC User's Guide* (MARC Analyses Research Corporation, Palo Alto 1996).
[34] *Physics of Group IV Elements and III-V Elements*, edited by K.-H. Hellwege, Landolt-Börnstein, New Series, Group III, Vol. 17, P. A (Springer-Verlag, Berlin, 1982).
[35] Q. K. K. Liu, N. Moll, M. Scheffler, and E. Pehlke, Phys. Rev. B **60**, 17008 (1999).
[36] Using the heat of evaporation of As_4 from As bulk, we estimate $\mu_{As}(T=500\ ^\circ C, p=8\times10^{-6}\ \text{mbar})=\mu_{As(bulk)}-0.25$ eV.
[37] E. Penev, P. Kratzer, and M. Scheffler, Phys. Rev. Lett. **93**, 146102 (2004).
[38] E. Penev, P. Kratzer, and M. Scheffler (unpublished).
[39] L. Geelhaar, J. Márquez, P. Kratzer, and K. Jacobi, Phys. Rev. Lett. **86**, 3815 (2001).
[40] D. B. Migas, S. Cereda, F. Montalenti, and L. Miglio, Surf. Sci. **556**, 121 (2004).
[41] O. E. Shklyaev, M. J. Beck, M. Asta, M. J. Miksis, and P. W. Voorhees, Phys. Rev. Lett. **94**, 176102 (2005).
[42] G.-H. Lu and F. Liu, Phys. Rev. Lett. **94**, 176103 (2005).
[43] G.-H. Lu, M. Cuma, and F. Liu, Phys. Rev. B **72**, 125415 (2005).
[44] I. Daruka and J. Tersoff, Phys. Rev. B **66**, 132104 (2002).
[45] P. B. Joyce, T. J. Krzyzewski, G. R. Bell, T. S. Jones, S. Malik, D. Childs, R. Murray, Phys. Rev. B **62**, 10891 (2000).
[46] E. Placidi *et al.*, Appl. Phys. Lett. **86**, 241913 (2005).
[47] M. C. Xu, Y. Temko, T. Suzuki, and K. Jacobi, Surf. Sci. **589**, 91 (2005).
[48] D. E. Jesson, G. Chen, K. M. Chen, and S. J. Pennycook, Phys. Rev. Lett. **80**, 5156 (1998).
[49] D. J. Vine, D. E. Jesson, M. J. Morgan, V. A. Shchukin, and D. Bimberg, Phys. Rev. B **72**, 241304(R) (2005).